Organic & Biomolecular Chemistry

www.rsc.org/obc

Volume 11 | Number 8 | 28 February 2013 | Pages 1261–1424

ISSN 1477-0520

RSC Publishing

PAPER

Goran Angelovski *et al.*

Synthesis and characterization of pH-sensitive, biotinylated MRI contrast agents and their conjugates with avidin

1477-0520(2013)11:8;1-B

Organic & Biomolecular Chemistry

RSC Publishing

PAPER

View Article Online
View Journal | View Issue

Cite this: *Org. Biomol. Chem.*, 2013, **11**, 1294

Synthesis and characterization of pH-sensitive, biotinylated MRI contrast agents and their conjugates with avidin†

Sandip M. Vibhute,[a] Jörn Engelmann,[b] Tatjana Verbić,[c] Martin E. Maier,[d] Nikos K. Logothetis[a,e] and Goran Angelovski*[a]

Responsive or smart contrast agents (SCAs) provide new opportunities in magnetic resonance imaging (MRI) to examine a number of physiological and pathological events. However, their application *in vivo* remains challenging. Therefore, much research is focused on the optimization of their properties, to enable their use in additional imaging modalities, pre-targeted delivery, or to increase the local concentration of the agent. The key feature in the SCA synthetic modification is the retention of their physicochemical properties related to the specific MR response. Here, we report the preparation and characterization of pH sensitive SCAs appended with a phosphonate pendant arm and either an aliphatic (**GdL^1**) or aromatic linker (**GdL^2**). The longitudinal relaxivity of **GdL^1** and **GdL^2** increases by 146% and 31%, respectively, while the pH decreases from 9 to 5. These two SCAs were converted to the biotinylated systems **GdL^3** and **GdL^4** and their interaction with avidin was investigated. The binding affinity with avidin was assessed with a fluorescence displacement assay and with MRI phantom experiments in a 3T MRI scanner. The fluorometric assay and MRI E-titrations revealed a 3 : 1 binding mode of **GdL$^{3–4}$** to avidin with the binding affinity as high as that of the parent avidin–biotin complex. The high binding affinity was confirmed with MRI by a competitive assay. The avidin–**GdL$^{3–4}$** complexes thus obtained exhibit changes in both r_1 and r_2 that are pH dependent. The results reveal a new pathway for the modification and improvement of SCAs to make them more suitable for *in vivo* application.

Received 6th August 2012,
Accepted 15th November 2012

DOI: 10.1039/c2ob26555a

www.rsc.org/obc

Introduction

Magnetic resonance imaging (MRI) has become an essential tool of medical diagnostic imaging and basic research over the past few decades. MRI has numerous advantages over other imaging techniques because of its high spatiotemporal resolution, non-invasiveness and non-ionizing signals.[1] Up to 45% of clinical MRI studies are performed using contrast agents, employed to enhance image quality.[2] The majority of MRI contrast agents are based on paramagnetic metal ions such as Mn^{2+} and Gd^{3+}, or superparamagnetic iron oxide nanoparticles (SPION).[3] Among these, the Gd^{3+}-systems are the most frequently used due to the high magnetic moment, and its long electronic spin relaxation time (10^{-9} s). In the presence of Gd^{3+}-agents, the relaxation rate of water protons increases resulting in an increased image contrast. The efficiency of a contrast agent (termed the longitudinal relaxivity, r_1) depends on many parameters such as number of directly bound water molecules to metal center *i.e.* hydration number (q), mean residence lifetime of the bound water molecules (τ_m), electron spin correlation time (T_{1e}), rotational correlation time (τ_r).[4] The tuning of such parameters can enhance the relaxivity of a given Gd^{3+}-based contrast agent, hence the resulting signal in an MR image.

Recently there is a growing trend to explore responsive or smart contrast agents (SCAs) which are able to report physiological changes in the region of interest, allowing noninvasive imaging of a specific biological process. There are many

[a]*Department for Physiology of Cognitive Processes, Max Planck Institute for Biological Cybernetics, Spemannstr. 38, 72076 Tübingen, Germany. E-mail: goran.angelovski@tuebingen.mpg.de; Fax: +49 7071 601 919; Tel: +49 7071 601 916*
[b]*High-Field Magnetic Resonance Center, Max Planck Institute for Biological Cybernetics, Tübingen, Germany*
[c]*Department of Analytical Chemistry, Faculty of Chemistry, University of Belgrade, Belgrade, Serbia*
[d]*Institute for Organic Chemistry, Faculty of Science, University of Tübingen, Tübingen, Germany*
[e]*Imaging Science and Biomedical Engineering, University of Manchester, Manchester, UK*

†Electronic supplementary information (ESI) available: HPLC elution conditions, fluorescence assay calculations and additional MRI phantom data. See DOI: 10.1039/c2ob26555a

different types of SCAs reported so far; those sensitive to a particular enzyme, pH, metal ion concentrations, or partial oxygen pressure.[5,6] Significant efforts have been undertaken by researchers to develop pH responsive agents, since changes in pH are associated with a number of physiological and pathophysiological processes.[7,8] These SCAs contain functional groups which change their protonation state around neutral pH, such as phosphonates or arylsulphonamides. The general mechanism reported so far involves alteration of the coordination environment around the metal center at different pH, which affects the number of proximate water molecules resulting in a change in the signal. The first pH responsive agent based on phosphonates was reported by Sherry and co-workers more than a decade ago.[9] In this SCA, hydrogen bonds formed after protonation of the phosphonate play a crucial role catalyzing the exchange of protons between inner and outer sphere water, resulting in a change in the signal at different pH. The sulfonamide based agent operates differently: at acidic pH the protonation of the nitrogen allows water to approach Gd^{3+}, whereas at basic pH deprotonation of nitrogen results in its coordination to the metal center, reducing q and hence relaxivity by hindering the access of water molecules to the inner sphere.[10]

However there is an upmost need for SCA with a response that can be combined with additional properties such as controlled biodistribution or determination of its exact local concentration. Such requirements necessitate additional synthetic modifications on SCAs and therefore special attention should be paid towards the changes in the physico-chemical properties of SCAs, to ensure their relaxivity changes, along with crucial issues such as the kinetic and thermodynamic stability, are retained. For instance, the *in vivo* biodistribution of probes varies considerably with slight changes in their structures.[11,12]

Proceeding in this direction, Sherry and co-workers attached a modified version of the previously mentioned phosphonate containing SCA to a PAMAM G5 dendrimer to improve the MR signal by increasing the molecular weight of the conjugate.[13] The relaxivity of the conjugate increased twice from pH 6 to pH 9.6 due to the increase in τ_r. However, due to its isoelectric point at pH $\sim$ 6, this dendrimeric SCA precipitates from solution. In another approach, a dual-modal MR-PET agent was prepared in which quantification of the local probe concentration was accomplished by the presence of the PET active ^{18}F nucleus, with the phosphonate-containing SCA, enabling pH mapping.[14] Other attempts involved modification of the sulfonamide based pH sensitive agent. Namely, the accessibility of its phenolic oxygen allowed the coupling of the functional molecule to a poly-β-cyclodextrin containing ^{19}F reporter. Here an adamantane derivative was introduced on the phenolic oxygen to achieve effective non-covalent coupling to the poly-β-cyclodextrin, where detection of the ^{19}F signal intensity is used to quantify the amount of the SCA.[15]

Our group recently reported a DO3A based, pH responsive probe appended with a phosphonate arm (DO3APP).[16] It was shown that coordination of the phosphonate arm to the metal center results in a decrease in pH. In this work, we report further synthetic modifications on the propylphosphonate containing SCA which involve the introduction of a side linker to allow the coupling of SCA to a diverse range of functional molecules such as dendrimers, nanoparticles, proteins, peptides or fluorescent tags. Most significantly the physico-chemical properties of SCAs, in particular their responsiveness (the pH dependent r_1 changes), must be retained after coupling to the linker. Consequently, the properties of SCAs and the other functional molecules could be used together to further characterize the function of the SCA *in vitro* and *in vivo*, broadening the scope of their application.

For this purpose we have designed two novel cyclen-based ligands $\mathbf{L^1}$ and $\mathbf{L^2}$ (Scheme 1). Their synthesis involved incorporating aliphatic (derivative of 6-aminohexanoic acid) and aromatic linkers (derivative of 4-(*p*-amino phenyl) butyric acid) onto cyclen derivatives ultimately producing ligands $\mathbf{L^1}$ and $\mathbf{L^2}$ respectively. These linkers were added on the cyclen nitrogen positioned *trans* to the propylphosphonate pendant arm, thus keeping these two pendant moieties as distant as possible to avoid any interference in the desired activity. Both linkers possess a primary amine as the terminal group, suitable for coupling to molecules containing free carboxylic acids, or electrophilic groups. Moreover, the aniline group in $\mathbf{L^2}$ can be converted to an isothiocyanate to enable further coupling to molecules with free amines. To demonstrate the applicability of the newly developed SCA, we incorporated biotin and studied the properties of the biotinylated SCA and their avidin conjugates regarding a pH-response. The biotin–avidin system has a specific interaction with an extraordinary affinity, being stable over larger range of pH and temperatures *in vivo*.[17] This system is thus an excellent tool for the targeted delivery of the SCA *in vivo*.

Results and discussion

Synthesis

$\mathbf{L^1}$ and $\mathbf{L^2}$ were obtained using two similar synthetic routes that commenced with the preparation of the two side arms (Scheme 1). Aliphatic brominated linker **2** was prepared by the diazotization of H-Lys(Z)-OH with sodium nitrite, followed by the bromination using potassium bromide and *tert*-butyl protection of carboxylic acid with 2,2,2-trichloroacetimidate.[18] 1,7-Bis(*tert*-butoxycarbonylmethyl)-1,4,7,10-tetraazacyclododecane (bis-*tert*-butyl DO2A) **6** was prepared following the procedure reported previously.[19] The key reaction of the synthesis was the selective mono-alkylation of **6** with the newly synthesized bromide **2** to obtain the tris-alkylated cyclen derivative **7**, achieved under high dilution in acetonitrile, using sodium bicarbonate. The final alkylation of **7** was achieved using diethyl(3-bromopropyl) phosphonate in acetonitrile in the presence of potassium carbonate to afford **8** in good yields. Hydrogenation of **8** with Pd/C and H_2 in ethanol gave primary amine **9**. Treatment of **9** with bromotrimethylsilane and subsequently formic acid yielded the ligand $\mathbf{L^1}$.

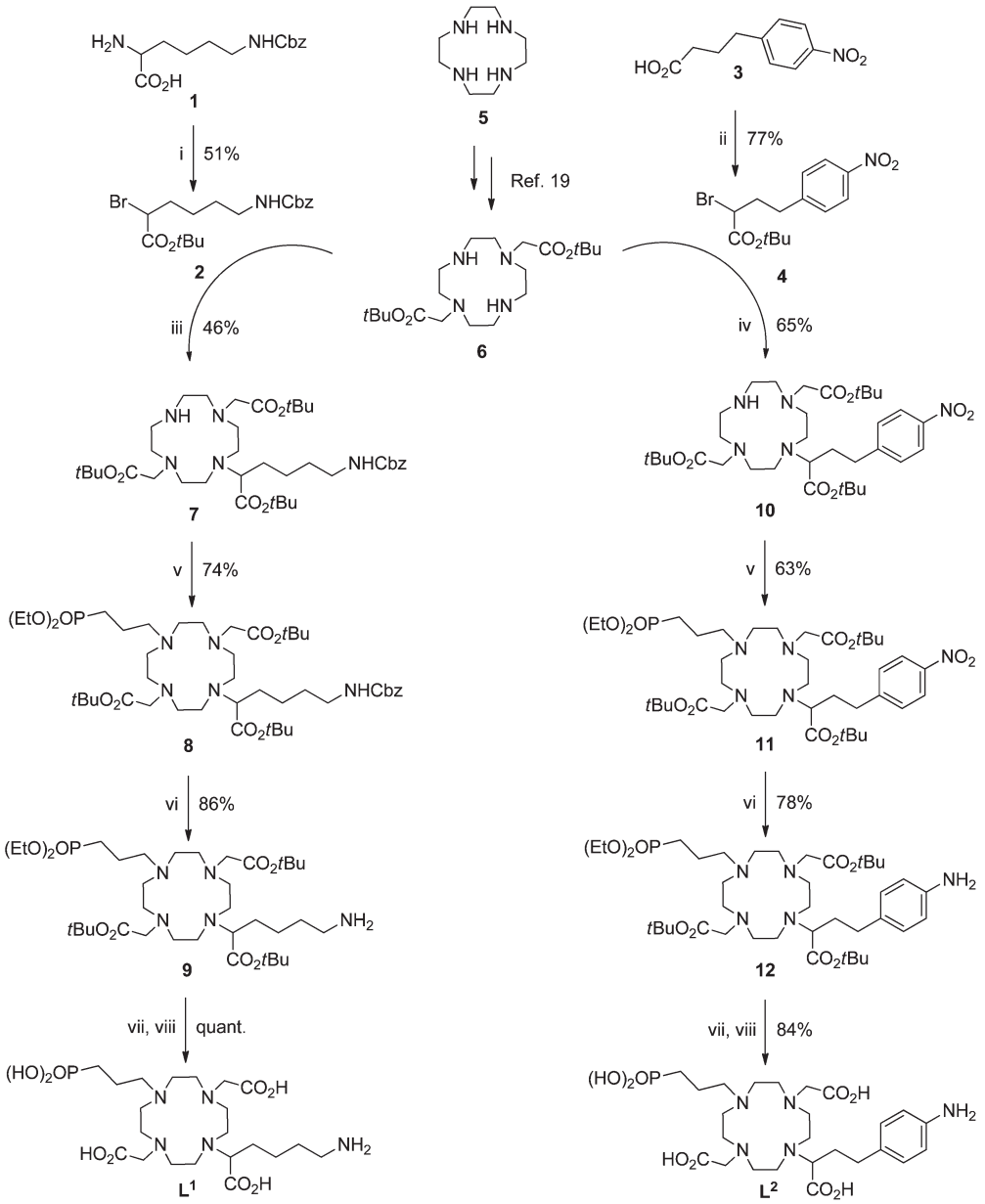

Scheme 1 Synthesis of $\mathbf{L^1}$ and $\mathbf{L^2}$. *Reagents and conditions*: (i) $NaNO_2$, KBr, 1N HBr, *t*-butyl-2,2,2-trichloroacetimidate, $CHCl_3$; (ii) $SOCl_2$, Br_2, *t*-butyl-2,2,2-trichloroacetimidate, $CHCl_3$; (iii) $NaHCO_3$, CH_3CN; (iv) $NaHCO_3$, CH_3CN; (v) diethyl (3-bromopropyl) phosphonate, K_2CO_3, CH_3CN; (vi) H_2, Pd/C, EtOH; (vii) $BrSi(CH_3)_3$, CH_2Cl_2, (viii) formic acid (for $\mathbf{L^1}$) or TFA (for $\mathbf{L^2}$), CH_2Cl_2.

The aromatic linker **4** was prepared according to a modified literature procedure,[20] achieving a higher yield (77% *vs.* 48%) than previously reported.[21] Selective monoalkylation of **6** was achieved following the same procedure as described for the aliphatic analogue **7**, to afford the nitro derivative **10**. The final alkylation of **10** with diethyl(3-bromopropyl) phosphonate resulted in **11**. The nitro group was converted into the amine **12** by hydrogenation using Pd/C as a catalyst in ethanol. Deprotection was carried out as described for $\mathbf{L^1}$ to afford $\mathbf{L^2}$, except that TFA was used instead of formic acid. Both ligands $\mathbf{L^1}$ and $\mathbf{L^2}$ were characterized by means of ^1H, ^{13}C, ^{31}P NMR and HR-ESI mass spectrometry.

Complexation of ligands $\mathbf{L^1}$, $\mathbf{L^2}$ with lanthanide chlorides ($GdCl_3{\cdot}6H_2O$, $EuCl_3{\cdot}6H_2O$) was carried out using a standard procedure (see the Experimental section) to obtain the desired complexes at neutral pH. The successful formation was confirmed by means of ESI-MS and the spectra contained appropriate isotope pattern distribution characteristic for Gd^{3+} or Eu^{3+} complexes.

Relaxometric and luminescence emission experiments

A relaxometric study of complexes $\mathbf{GdL^{1-2}}$ was performed at 7 T (300 MHz) and 25 °C. The T_1 relaxation times were recorded at pH 9, 7 and 5 using different concentrations of

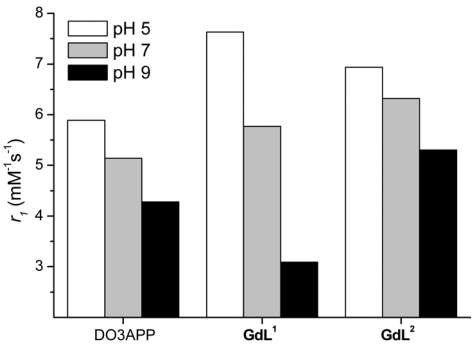

Fig. 1 The pH dependence of the proton relaxivity (r_1) of **GdL^1** and **GdL^2** (7 T, 25 °C) compared to DO3APP[16] (7 T, 21 °C).

Table 1 Emission lifetimes and estimated q values of **EuL^1** at neutral and acidic pH/pD

Compound	τ (ms) H_2O	τ (ms) D_2O	q
pH/pD 7	0.56	1.69	**1.1**
pH/pD 5	0.42	1.51	**1.8**

complexes. The pH was adjusted using solid lithium hydroxide and *para*-toluenesulfonic acid to avoid dilution of **GdL$^{1-2}$** solutions. The exact concentration of Gd^{3+} was determined by the bulk magnetic susceptibility shift method.[22] The r_1 relaxivity at each pH is obtained as a slope of the linear regression curve for concentrations of **GdL$^{1-2}$** plotted against the relaxation rate (R_1). The relaxivities of both **GdL$^{1-2}$** at the acidic pH were slightly higher than for the parent DO3APP compound (Fig. 1).[16] In both cases we observed a continuous increase in relaxivity from pH 9 to 5. A total increase in r_1 of 147% from pH 9 to pH 5 was recorded for **GdL^1** (32% from pH 7 to pH 5), whilst a total increase of 31% in r_1 was observed for **GdL^2** over the same pH range. The change in relaxivity with a change in pH is observed as in the parent compound. Protonation of the phosphonate in acidic pH induces movement of the pendant arm from the metal center and allows more water molecules to interact with the metal center resulting in a higher relaxivity.

$$q = A' (\Delta\, k_{H_2O} - \Delta\, k_{D_2O} - 0.25) \quad (1)$$

The two responsive complexes were characterized further by investigating their Eu^{3+} analogues. The ^{31}P NMR spectra of **EuL^1** and **EuL^2** were recorded at pD 5 and 7. A pH-dependent low field chemical shift of approximately 2 ppm in both complexes indicates that a similar mechanism responsible for the r_1 changes is occurring as observed for DO3APP.[16] Time resolved luminescence decay experiments were performed on complexes **EuL^1** and **EuL^2** to evaluate the change in the inner sphere hydration at different pH (Table 1). The experiments were carried out in 5 mM solutions of **EuL$^{1-2}$** in H_2O and D_2O. The hydration number was estimated using eqn (1) where A' is 1.2 ms and the correction factor for the contribution of the second sphere is -0.25 ms^{-1}.[23]

For **EuL^1** the apparent q value increases from 1.1 to 1.8 as the pH decreases from 7 to 5. The observed change is in good agreement with the findings of relaxivity experiments on the corresponding Gd^{3+} complex, confirming that the change in r_1 is directly influenced by changes in q.

Determination of the q value for **EuL^2** was not possible due to the low intensity of emission and low solubility of the complex at high concentrations (>3–4 mM). One of the reasons for the weak emission could be the presence of the highly electron donating aniline derivative in close proximity of the metal center which quenches the signal, whereas the hydrophobic aromatic ring of the linker might decrease the solubility.[24]

The relaxometric and luminescence emission experiments performed on the modified phosphonate complexes confirm that the synthetic modifications in close proximity of the metal centre do not negatively affect the coordination of Ln^{3+}, hence the pH responsive properties (similar to the DO3APP parent compound) are retained. This enabled us to pursue further investigations involving **L$^{1-2}$** towards their potential MRI application with other biomolecules such as proteins (see below).

Biotinylation of GdL$^{1-2}$

The high affinity avidin–biotin conjugate is a widely studied system used in many therapeutic, diagnostic, and pharmacological applications.[25–27] Avidin is a tetrameric protein with a high molecular mass (66 k Dalton) and has an extremely high binding affinity towards biotin ($K_d \sim 1.7 \times 10^{-15}$) over wide pH range.[17] Once biotinylated, the avidin conjugate of our SCA can be delivered to specific regions *in vivo*, or the biotinylated SCA alone could be used for selective cell-targeting.[28] Hence, we have synthesized two biotinylated molecules **L^3** and **L^4** in a two step procedure commencing with the ester-protected ligands **9** and **12** (Scheme 2). They were coupled to biotin using EDCI·HCl and DMAP in DMF at room temperature, where the reaction was monitored by ESI-MS. The ligands were obtained following the deprotection of phosphonate and carboxylic acids using bromotrimethylsilane and trifluoroacetic acid respectively. Upon characterization of the ligands, their Gd^{3+} complexes were prepared as described previously (see above and the Experimental section).

Fluorescence displacement assay

The binding affinity of the newly synthesized molecules **GdL$^{3-4}$** to avidin was measured using a fluorometric assay based on the displacement of the fluorescent probe 2-anilinonaphthalene-6-sulfonic acid (ANS), employing the method developed by Horowitz and coworkers.[29] Briefly, ANS is strongly fluorescent when attached to avidin whereas the unbound dye has only a low fluorescence intensity. Since the binding affinity of ANS to avidin is lower than binding affinity of biotin to avidin, the addition of biotin displaces ANS from the avidin binding pocket resulting in the quenching of the fluorescence in the sample.

The fluorescence displacement assay was performed in parallel on biotin, **GdL^3** and **GdL^4**. Upon addition of biotin or a biotinylated probe to the mixture of avidin and ANS, the

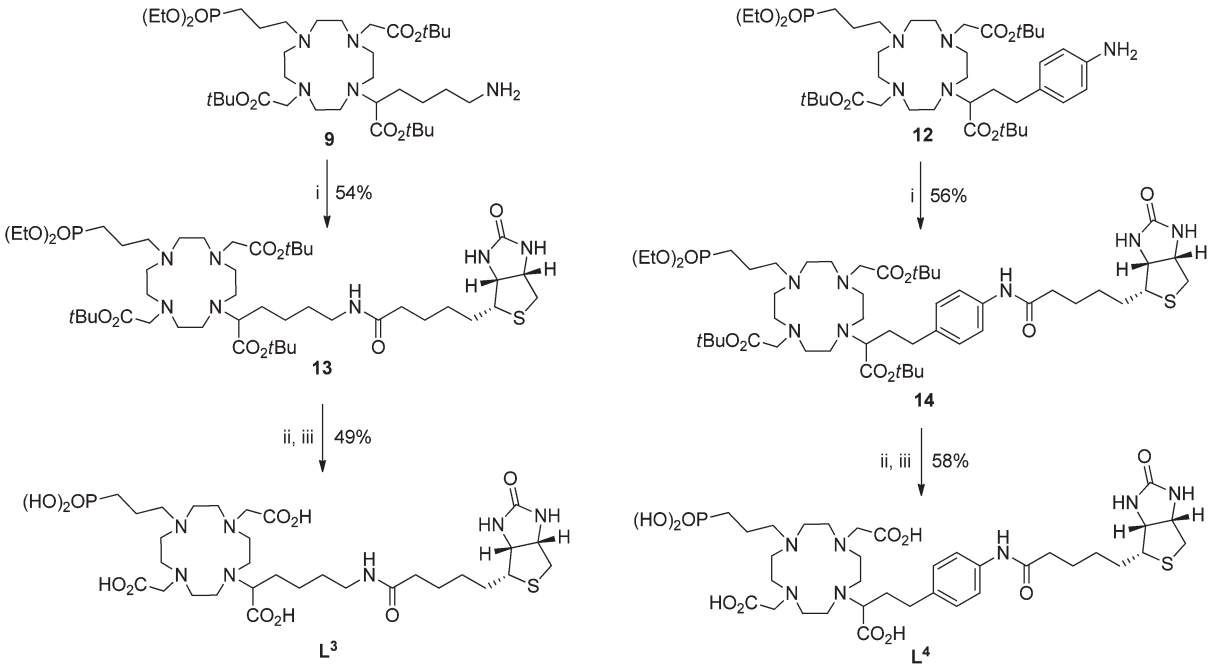

Scheme 2 Synthesis of $\mathbf{L^3}$ and $\mathbf{L^4}$. *Reagents and conditions*: (i) biotin, EDCI·HCl, DMAP, DMF; (ii) $BrSi(CH_3)_3$, CH_2Cl_2; (iii) TFA, CH_2Cl_2.

fluorescence intensity decreased reaching a sharp inflection point at 3 equiv. of biotin or $\mathbf{GdL^{3-4}}$ (Fig. S1, ESI†). After this point there was no further drop in intensity observed even after the addition of several equivalents of biotin or $\mathbf{GdL^{3-4}}$. The measured stoichiometry is in line with the results previously reported by Horowitz and can be associated with the affinity-purified avidin obtained from commercial sources.[29] This assay shows that only three binding sites are available in the studied avidin to interact with ANS and these three molecules of dye can be replaced by biotin or biotinylated SCA. However, the titration curves of $\mathbf{GdL^{3-4}}$ are comparable to biotin indicating that the binding affinities of both compounds are as strong as biotin. The calculated stability constants with K_s values 5.1×10^{13}, 7.1×10^{13} and 8.0×10^{13} for biotin, $\mathbf{GdL^3}$ and $\mathbf{GdL^4}$, respectively, suggest that the binding affinities of biotin and biotinylated SCA are not significantly different from each other (see ESI†).

MRI phantom experiments

To confirm the observations from the fluorescence displacement assays, we followed the longitudinal and transverse relaxation rates (R_1, R_2) in samples with a constant concentration of $\mathbf{GdL^{3-4}}$ in HEPES buffer and varying concentrations of avidin in a method known as an E-titration.[30] These mixtures were incubated at 37 °C for 2 h and their relaxation times T_1 and T_2 were measured using a 3T (123 MHz) MRI scanner following the procedure and parameters as described in the Experimental section. A linear increase in r_1/r_2 with addition of avidin compared to the unbound probe was observed until all biotinylated complexes are bound to avidin. A further increase in avidin concentration has no further effect on r_1/r_2 (Fig. 2). The MRI phantom experiments confirm that biotinylated complexes bind to avidin. The increase in the r_1/r_2 of conjugates is the direct consequence of the τ_R decrease, which is commonly observed for macromolecular contrast agents at magnetic fields relevant for clinics.[31] The plateaus of r_1/r_2 values were observed at 0.3–0.4 equiv. of avidin which matches our observations from the fluorometric assay, indicating that three of the binding sites are occupied in avidin.

In the subsequent step we studied the pH response of $\mathbf{GdL^{3-4}}$ in the absence and presence of avidin. We mixed $\mathbf{GdL^{3-4}}$ and avidin in a 3 : 1 ratio. The pH was adjusted over the wide range starting from 5.5 to 9.0 using different buffers (25 mM). Longitudinal T_1 and transverse T_2 relaxation times were again obtained at 25 °C in a 3T MRI scanner.

A decrease in relaxation times T_1 and T_2, hence an increase in r_1 and r_2, was observed for both complexes when the pH decreased from 9.0 to 5.5 (Fig. 3). A good reproducibility was observed over five independent experiments performed. The $\mathbf{GdL^3}$–avidin conjugate showed an increase from 10.4 to 12.6 mM^{-1} s^{-1} (21%) and from 39.3 to 58.4 mM^{-1} s^{-1} (49%) of r_1 and r_2 respectively. Within the same pH range, the $\mathbf{GdL^4}$–avidin conjugate showed an increase from 11.2 to 12.6 mM^{-1} s^{-1} (12%) and from 40.4 to 52.6 mM^{-1} s^{-1} (30%) of r_1 and r_2 respectively. When comparing these values with those obtained under same conditions (3T scanner, pH 5.5–9.0) for $\mathbf{GdL^{3-4}}$ in the absence of avidin, the relative changes in relaxivities are comparable, except that the absolute r_2 values are much higher in the $\mathbf{GdL^{3-4}}$–avidin conjugates (Fig. 3 and S3–S4 in ESI†). The results suggest that the investigated SCA remained responsive not only by the further synthetic modifications (biotinylation of $\mathbf{GdL^{1-2}}$ to $\mathbf{GdL^{3-4}}$), but $\mathbf{GdL^{3-4}}$ are capable of a specific and strong binding to the avidin while retaining their MR activity. Finally, the observed r_1/r_2 changes

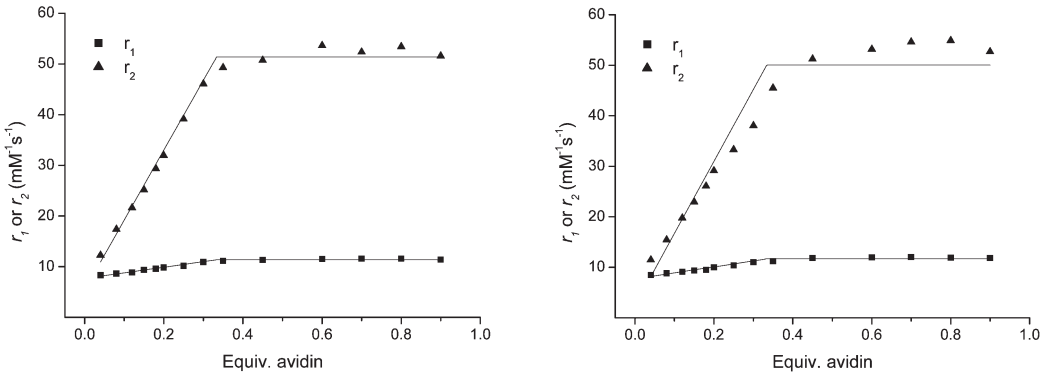

Fig. 2 E-titrations of **GdL^3** (left) and **GdL^4** (right) with avidin at a 3T MRI scanner (21 °C, HEPES, pH 7.4). The lines correspond to the fit assuming $n = 3$ and K_s^{II} (Av(**GdL^3**)$_3$) = 7.1×10^{13} or K_s^{II} (Av(**GdL^4**)$_3$) = 8.0×10^{13} obtained from the fluorescence displacement assay. The R^2 values were 0.9817 and 0.9924 for r_1 and r_2 respectively for **GdL^3**, whereas 0.9583 and 0.9438 for r_1 and r_2 respectively for **GdL^4**. A better fit (R^2 = 0.9936 and 0.9963 for r_1 and r_2 respectively) for **GdL^4** could be obtained when n is also fitted (n = 2.4 and 2.3 for r_1 and r_2 respectively). The fitting equation is described in ESI†.

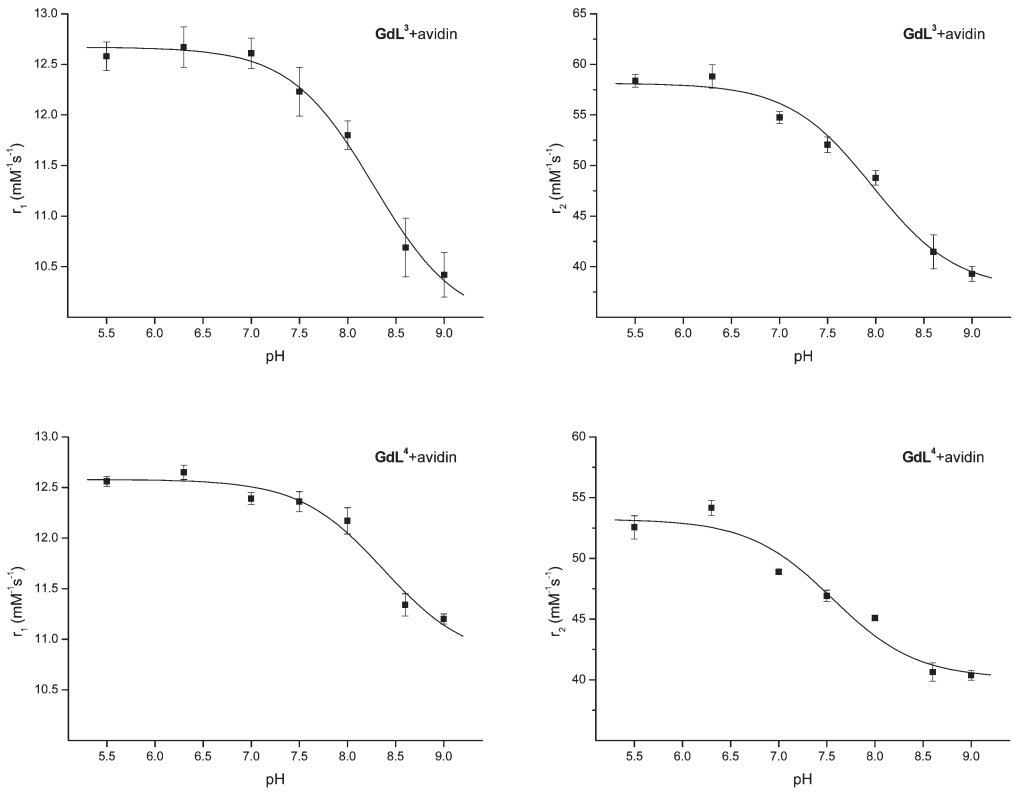

Fig. 3 pH-dependent r_1 (left) and r_2 (right) response of **GdL^3** (top) and **GdL^4** (bottom) with avidin at a 3T MRI scanner (21 °C). The avidin : **GdL$^{3-4}$** molar ratio was 1 : 3. Values are presented as mean ± SEM of five independent experiments. The lines represent the result of the sigmoidal fit and are displayed to aid a better visualization of the pH dependent r_1/r_2 decrease.

are the most pronounced in the pH range 7.0 to 8.5, making **GdL$^{3-4}$** a promising prototype SCA for further investigations *in vivo* under physiological conditions.

Competitive MRI assay

We performed a competitive assay with biotin to further characterize the binding affinity of the biotinylated SCA towards avidin and estimate their *in vivo* potency. **GdL$^{3-4}$** was mixed with avidin in a fixed 3 : 1 ratio (HEPES buffer, pH 7.4). Different concentrations of biotin were added and the mixtures were incubated for five hours. If the binding affinity of the SCA is lower than biotin, **GdL$^{3-4}$** should be displaced by biotin from the avidin binding pocket, resulting in a decrease in relaxivity, in particular r_2. Following the incubation, the longitudinal and transverse relaxation times were measured in a 3T MRI scanner. We observed a minor decrease in relaxivities

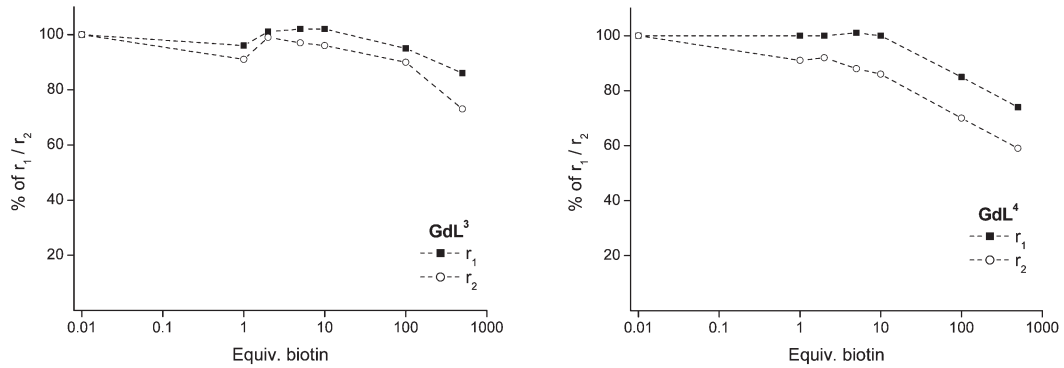

Fig. 4 Competitive MRI assay of avidin : **GdL^3** (1 : 3, 125 μM **GdL^3**, left) and avidin : **GdL^4** (1 : 3, 125 μM **GdL^4**, right) with varying concentrations of biotin at a 3T MRI scanner (21 °C).

only after addition of 100 times excess of biotin whereas the r_1/r_2 did not change at lower concentrations of biotin (Fig. 4). Such results are expected given the equilibrium exchange of biotinylated **GdL$^{3-4}$** at high concentrations of biotin. However, these findings confirm that the binding affinity of **GdL^3** and **GdL^4** to avidin is as high as that of biotin. Furthermore, they imply the stability of MRI signal changes caused by the SCA either in its premixed solution with biotin or in the presence of endogenous biotin *in vivo*.

Conclusions

In conclusion, we have synthesized and characterized two novel macrocyclic gadolinium based pH responsive contrast agents with an aliphatic or aromatic linker. Relaxometric and luminescence studies at different pH confirmed that for both agents the main physicochemical properties related to the pH dependent MRI response were retained after inserting the linking unit and are comparable to their parent compound. Furthermore, they were coupled to biotin and the response of the newly prepared responsive MRI agents was studied in more detail. The binding affinity of these complexes with avidin was shown to be as effective as biotin itself through fluorescence displacement or competitive MRI assays. MRI phantom experiments in the presence of avidin revealed that the relaxivity was changing along with the change in pH at physiologically relevant values. These complexes offer a useful pathway towards target-specific SCAs for *in vivo* applications. Future directions will involve applying this strategy in introducing various functional molecules such as proteins, peptides, receptor ligands or fluorescent tags to SCAs of various kinds (*e.g.* pH- or ion-responsive) making them suitable for their application *in vivo*.

Experimental section

General remarks

All chemicals were purchased from commercial sources and used without further purification. H-Lys(Z)-OH (**1**), 4-(4-nitro phenyl butyric acid (**3**) and biotin were purchased from Sigma-Aldrich, Germany. Cyclen (**5**) was purchased from CheMatech, France. Avidin was purchased from Merck, Germany. ANS was purchased from Life Technologies GmbH, Germany. Column chromatography was performed using silica gel 60 (70–230 mesh ASTM) or aluminium oxide 90 active basic from Merck (Germany). Reversed-phase high-performance liquid chromatography was performed on a Varian PrepStar Instrument (Australia), equipped with PrepStar SD-1 pump heads. Analytical RP-HPLC was performed on the Atlantis C18 column 4.6 mm × 150 mm, particle size 5 μm and semi-preparative RP-HPLC was performed on the Atlantis C18 column 19 mm × 150 mm, particle size 5 μm (Waters Corporation, USA) using elution conditions described as in the ESI (Table S1†).

^{1}H, ^{13}C {1H}, ^{31}P {1H} NMR spectra and relaxometric experiments were recorded on a Bruker Avance III 300 MHz 'Microbay' spectrometer (Bruker, Germany). ESI-LRMS were performed on an ion trap SL 1100 system (Agilent, Germany). FT-ICR-MS were performed on a Bruker FT-ICR Apex II spectrometer (Bruker, Germany). HR-EI-MS were performed on a MAT Sektorfeld mass spectrometer (Finnigan, Germany). Luminescence steady-state and time resolved measurements were performed on a QuantaMaster™ 3 PH fluorescence spectrometer from Photon Technology International, Inc. (USA).

Synthetic procedures

***tert*-Butyl-6-(((benzyloxy)carbonyl)amino)-2-bromohexanoate (2).** Potassium bromide (2.96 g, 12.50 mmol) was added to the solution of H-Lys(Z)-OH (2.00 g, 7.13 mmol) in HBr (16 mL, 1 N). The resulting mixture was cooled to 0 °C, sodium nitrite (0.59 g, 8.56 mmol) was added portionwise over 1 h and the mixture was stirred for a further 2 h. Conc. sulfuric acid (1 mL) was added slowly at 0 °C and the solution was allowed to reach room temperature. The mixture was extracted with diethyl ether (3 × 150 mL). The combined organic layers were dried over anhydrous sodium sulphate and concentrated to afford a bromo derivative of acid as a light yellow syrup. This acid (0.50 g, 1.45 mmol) was suspended in chloroform (5 mL) and *tert*-butyl-2,2,2-trichloroacetimidate (0.64 g, 2.90 mmol) in

chloroform (5 mL) was added dropwise. After 10 minutes a catalytic amount of trifluoroborane diethyl etherate (10 μL) was added and the resulting mixture was stirred at room temperature for 16 h under a nitrogen atmosphere. Sodium bicarbonate (1.00 g) was added to the mixture and stirred for another 10 minutes. The insoluble salts were removed by filtration and the residue was obtained after concentration of the filtrate. The residue was purified using silica gel column chromatography (6% ethyl acetate/hexane) to obtain a light yellow semi-solid of **2** (0.30 g, 51%).

^{1}H NMR (300 MHz, $CDCl_3$) δ (ppm): 1.41–1.63 (m, 13H, $CH_2CH_2CH_2CH_2$, $(CH_3)_3C$), 1.87–2.12 (m, 2H, $CH_2CHBrCO$), 3.19 (t, J = 6 Hz, 2H, $NHCH_2CH_2$), 4.10 (t, J = 6 Hz, 1H, $CH_2CHBrCO$), 4.84 (br s, 1H, $NHCH_2$), 5.10 (s, 2H, $PhCH_2OC(O)$), 7.37–7.32 (m, 5H, Ar*H*). ^{13}C{1H} NMR (75 MHz, $CDCl_3$) δ (ppm): 24.4 ($NHCH_2CH_2CH_2$), 27.7 ($(CH_3)_3C$), 29.2 ($CHBrCH_2CH_2$), 34.4 ($NCH_2CH_2CH_2$), 40.6 ($CHBrCH_2CH_2$), 47.4 ($COCHBrCH_2$), 66.6 ($PhCH_2OC(O)$), 82.4 ($(CH_3)_3C$), 128.1, 128.5, 136.5 (Ar*C*), 156.3, 168.7 (*C*(O)). ESI-HRMS: calculated for $C_{18}H_{26}BrNNaO_4$ $[M + Na^+]^+$, m/z 422.0937, found 422.0937.

***tert*-Butyl-2-bromo-4-(4-nitrophenyl)butanoate (4).** 4-(4-Nitrophenyl)-butyric acid (3.00 g, 14.34 mmol) was dissolved in thionyl chloride (4.16 mL, 57.36 mmol) and the mixture was stirred at 75 °C for 16 h. Bromine (0.82 mL, 15.78 mmol) was added dropwise at the same temperature and the mixture was again stirred for 16 h. The reaction mixture was cooled to room temperature and the mixture was poured over ice and stirred for 2 h. The aqueous layer was extracted with diethyl ether (3 × 200 mL). The combined organic phases were washed with brine (200 mL), dried over Na_2SO_4 and concentrated under reduced pressure. The residue was redissolved in chloroform (30 mL) and a solution of *tert*-butyl-2,2,2-trichloroacetimidate (6.27 g, 28.68 mmol) in chloroform (20 mL) was added slowly followed by boron trifluoride etherate (100 μL). The resulting mixture was stirred at room temperature for 16 h. Sodium bicarbonate (2.00 g) was added and stirred for 30 minutes. The inorganic impurities were removed by filtration, the filtrate was concentrated and the residue was purified by silica gel column chromatography (2% ethyl acetate/hexane) to afford a light yellow oil of bromide **4** as a pure product (3.80 g, 77%).

^{1}H NMR (300 MHz, $CDCl_3$) δ (ppm): 1.49 (s, 9H, $(CH_3)_3C$), 2.21–2.43 (m, 2H, CH_2CH_2CHBr), 2.77–3.00 (m, 2H, CH_2CH_2CHBr), 4.07 (dd, J = 9, 6 Hz, 1H, CH_2CH_2CHBr), 7.38 (d, J = 9 Hz, 2H, Ar*H*), 8.18 (d, J = 9 Hz, 2H, Ar*H*). ^{13}C{1H} NMR (75 MHz, $CDCl_3$) δ (ppm): 27.7 ($(CH_3)_3C$), 33.1 ($ArCH_2CH_2CHBr$), 35.7 ($ArCH_2CH_2CHBr$), 46.4 ($ArCH_2CH_2CHBr$), 82.8 ($(CH_3)_3C$), 123.9, 129.3, 146.7, 147.9 (Ar*C*), 168.3 (*C*(O)). ESI-HRMS for $C_{14}H_{18}BrNO_4$ $[M + Na]^+$, m/z calcd 366.0311, found 366.0307.

Compound 7. A solution of bromide **2** (2.00 g, 5.00 mmol) in anhydrous acetonitrile (50 mL) was added dropwise over 2 h to the mixture of **6**[19] (2.50 g, 6.25 mmol) and sodium bicarbonate (0.42 g, 5.00 mmol) in anhydrous acetonitrile (100 mL) at room temperature. The resulting mixture was stirred at room temperature for 2 days. Insoluble salts were removed by filtration and the filtrate was concentrated under reduced pressure. A pure product was afforded by silica gel column chromatography (3% methanol/dichloromethane) to give **7** as an off-white solid (1.65 g, 46%).

^{1}H NMR (300 MHz, $CDCl_3$) δ (ppm): 1.43 (m, 27H, $(CH_3)_3C$), 1.56–1.68 (m, 4H, $CH_2CH_2CH_2CH_2$), 2.32–3.53 (br, 21H, CH_2 ring, *C*HCOO*t*Bu and $CH_2COOtBu$), 5.06 (s, 2H, $PhCH_2CO$), 5.79 (br s, 1H, $CH_2NHCOOCH_2$), 7.19–7.39 (m, 5H, Ar*H*), 9.49 (br s, 1H, N*H* ring). ^{13}C{1H} NMR (75 MHz, $CDCl_3$) δ (ppm): 23.8, 28.1, 28.2 ($(CH_3)_3C$), 29.2, 30.0, 40.4 ($NHCH_2CH_2$), 45.6, 48.5, 49.9, 50.9 (CH_2 ring), 56.1 ($CH_2COOtBu$), 61.9 (*C*HCOO*t*Bu), 66.1 ($PhCH_2OC(O)$), 81.5, 81.7, ($(CH_3)_3C$), 127.7, 127.8, 128.3, 136.9 (Ar*C*), 156.6, 170.1, 171.4 (*C*(O)). ESI-HRMS: calculated for $C_{38}H_{66}N_5O_8$ $[M + H^+]^+$, m/z 720.4911, found 720.4901.

Compound 8. Potassium carbonate (0.27 g, 1.99 mmol) and diethyl (3-bromopropyl) phosphonate (0.38 mL, 1.99 mmol) were added to the solution of compound **7** (1.30 g, 1.80 mmol) in anhydrous acetonitrile (15 mL). The reaction mixture was heated to 70 °C for 16 h. The insoluble solids were removed by filtration, the filtrate was concentrated under reduced pressure and the residue was purified by silica gel column chromatography (50% methanol/dichloromethane/10% ammonia). Removal of solvents yielded a light yellow oil of **8** (1.20 g, 74%).

^{1}H NMR (300 MHz, $CDCl_3$) δ (ppm): 1.29 (t, J = 6 Hz, 6H, OCH_2CH_3), 1.36–1.80 (m, 37H, $CH_2CH_2P(O)$, $(CH_3)_3C$), 2.28–2.94 (br, 18H, CH_2 ring), 3.12–3.22 (m, 7H, *C*HCOO*t*Bu and $CH_2COOtBu$), 4.94–4.17 (m, 4H, $POCH_2$), 5.07 (s, 2H, $PhCH_2OC(O)$), 5.46 (br s, 1H, CH_2NHCbz), 7.21–7.42 (m, 5H, Ar*H*). ^{13}C{1H} NMR (75 MHz, $CDCl_3$) δ (ppm): 16.3 (d, J = 6 Hz, OCH_2CH_3), 20.2 (d, J = 4.5 Hz, $P(O)CH_2CH_2$), 23.3 (d, $^1J_{PC}$ = 141 Hz, $P(O)CH_2CH_2$), 23.3, 28.1, 28.2, 29.3, 29.5, 40.7 (CH_2CH_2NHCOO), 49.5 (NCH_2CH_2), 52.3, 52.5, 52.6, 56.0 (CH_2 ring), 61.2, 61.2 ($CH_2COOtBu$), 64.1 (*C*HCOO*t*Bu), 66.2 (OCH_2CH_3), 80.4, 80.5 ($(CH_3)_3C$), 127.8, 128.0, 128.3, 136.7 (Ar*C*), 156.3, 170.8, 172.8 (*C*(O)). ^{31}P{^{1}H} NMR (122 MHz, $CDCl_3$) δ (ppm): 32.9 (s). ESI-HRMS: calculated for $C_{45}H_{81}N_5O_{11}P$ $[M + H]^+$, m/z 898.5670, found 898.5659.

Compound 9. Compound **8** (0.68 g, 0.75 mmol) was dissolved in absolute ethanol (20 mL) and 10% Pd–C (70 mg, 10% w/w) was added. The heterogeneous mixture was shaken for 16 h under a hydrogen atmosphere (35 psi) in a Parr hydrogenator apparatus. The catalyst was removed by filtration through the celite and the filtrate was concentrated to obtain a light yellow oil of the amine **9** (0.50 g, 86%).

^{1}H NMR (300 MHz, $CDCl_3$) δ (ppm): 1.31 (t, J = 6 Hz, 6H, OCH_2CH_3), 1.37–1.95 (br, 37H, $P(O)CH_2CH_2CH_2$, $NHCH_2CH_2CH_2CH_2$, $(CH_3)_3C$), 2.15–3.45 (br, 25H), 3.95–4.20 (m, 4H, OCH_2CH_3). ^{13}C{1H} NMR (75 MHz, $CDCl_3$) δ (ppm): 16.5 (d, J = 6 Hz, OCH_2–CH_3), 20.0 (d, J = 4.5 Hz, $P(O)CH_2CH_2$), 23.5 (d, $^1J_{PC}$ = 140 Hz, $P(O)CH_2CH_2$), 23.6, 28.2, 28.3 ($(CH_3)_3C$), 29.9, 33.5, 42.1 ($CH_2CH_2NH_2$), 49.6 (NCH_2CH_2), 52.3, 52.3, 52.7, 56.2 (CH_2 ring), 61.3, 61.4 ($CH_2COOtBu$, OCH_2CH_3), 64.2 (*C*HCOO*t*Bu), 80.5, 80.6 ($(CH_3)_3C$), 171.0, 172.9 (*C*(O)). ^{31}P{^{1}H} NMR (122 MHz, $CDCl_3$) δ (ppm): 31.0 (s), 32.9 (s). ESI-HRMS:

calculated for $C_{21}H_{41}N_5O_9P$ $[M + H]^+$, *m*/*z* 764.5296, found 764.5294.

Ligand L[1]. Bromotrimethylsilane (0.62 g, 3.90 mmol) was added slowly at 0 °C to the solution of the amine **9** (0.30 g, 0.39 mmol) in anhydrous dichloromethane (20 mL). The reaction mixture was stirred for 12 h at room temperature. The solvent was removed under reduced pressure and the residue was dissolved in formic acid (4 mL) and stirred at 60 °C for 16 h. The reaction mixture was cooled to room temperature and excess volatiles were removed under reduced pressure. The residue was dissolved in water (2 mL) and added slowly to acetone (200 mL) under vigorous stirring. The solution was cooled to −20 °C for 12 h. The solid product was separated by filtration, dried under reduced pressure to afford an off-white solid of **L[1]** (0.30 g, quant.).

^{1}H NMR (300 MHz, D_2O) δ (ppm): 1.40–2.15 (br, 10H), 2.80–3.35 (br, 23H, CH_2 ring, CH_2 acid arm), 4.09 (m, 1H, NC*H*(COOH)CH_2). ^{13}C{1H} NMR (75 MHz, D_2O) δ (ppm): 17.2, 23.6, 23.6 (d, $^1J_{PC}$ = 137 Hz, P(O)*C*$H_2$$CH_2$), 24.8, 26.5, 39.0, 46.9, 47.2, 48.3, 49.6, 49.9, 50.0, 50.1, 53.3, 54.2, 54.4, 63.1 (*C*HCOOH), 170.8, 173.6, 174.58 (*C*(O)). ^{31}P{^{1}H} NMR (122 MHz, D_2O) δ (ppm): 27.2 (s). ESI-HRMS for $C_{21}H_{41}N_5O_9P$: $[M - H^+]^-$, *m*/*z* calcd 538.2647, found 538.2648.

Compound 10. Sodium bicarbonate (0.37 mg, 4.40 mmol) and a solution of bromide **4** (1.51 g, 4.40 mmol) in anhydrous acetonitrile (50 mL) were added slowly to a solution of bis-*tert*-butyl DO2A **6** (2.20 g, 5.50 mmol) in anhydrous acetonitrile (100 mL) over 3 h at room temperature. The resulting mixture was stirred at room temperature for 2 days. The inorganic impurities were removed by filtration, the filtrate was concentrated under reduced pressure and the residue was purified by silica gel column chromatography (3% methanol/dichloromethane). The product **10** was afforded as an off-white solid after recrystallization from cold diethyl ether (1.90 g, 65%).

^{1}H NMR (300 MHz, $CDCl_3$) δ (ppm): 1.40 (s, 9H, $(CH_3)_3C$) 1.49 (s, 18H, $(CH_3)_3C$), 1.93–2.25 (br, 2H, CHC$H_2$$CH_2$), 2.38 (d, *J* = 12 Hz, 2H, ArC$H_2$$CH_2$), 2.53–3.37 (br, 21H, C*H*COO*t*Bu and CH_2COO*t*Bu, CH_2 ring), 7.63 (d, *J* = 9 Hz, 2H, Ar*H*), 8.17 (d, *J* = 9 Hz, 2H, Ar*H*). ^{13}C{1H} NMR (75 MHz, $CDCl_3$) δ (ppm): 28.0, 28.3 ($(CH_3)_3C$), 31.6 (ArC$H_2$$CH_2$), 32.3 (ArC$H_2$$CH_2$), 45.8, 48.2, 49.5, 50.8 (*C*H_2 ring), 55.5 (*C*H_2COO*t*Bu), 60.3 (*C*HCOO*t*Bu), 81.6, 82.2 ($(CH_3)_3C$), 123.7, 130.1, 146.6, 148.9 (Ar*C*), 170.04, 170.9 (*C*(O)). ESI-HRMS for $C_{34}H_{57}N_5O_8$ $[M + H]^+$, *m*/*z* calcd 664.4279, found 664.4282.

Compound 11. Compound **10** (0.93 g, 1.40 mmol) was dissolved in anhydrous acetonitrile (20 mL) and potassium carbonate (0.23 g, 1.68 mmol), diethyl (3-bromopropyl) phosphonate (0.32 mL, 1.68 mmol) and catalytic amount of potassium iodide were added at room temperature. The resulting mixture was stirred at 70 °C for 16 h. After cooling to room temperature, the insoluble materials were removed by filtration, the filtrate was concentrated under reduced pressure to afford a residue which was purified by silica gel column chromatography (50% methanol/dichloromethane/2% ammonia) to obtain **11** as a light yellow oil (0.75 g, 63%).

^{1}H NMR (300 MHz, $CDCl_3$) δ (ppm): 1.30 (t, *J* = 7.5 Hz, 6H, P(O)OCH_2CH_3), 1.37–1.56 (m, 27H, $(CH_3)_3C$), 1.61–2.22 (br, 6H, ArCH_2CH_2, P(O)CH_2CH_2CH_2), 2.31–3.05 (br, 20H, CH_2 ring), 3.10–3.35 (m, 5H, C*H*COO*t*Bu, CH_2COO*t*Bu), 3.96–4.18 (m, 4H, OC$H_2$$CH_3$), 7.38 (d, *J* = 7.5 Hz, 2H, Ar*H*), 8.13 (d, *J* = 7.5, 2H, Ar*H*). ^{13}C{1H} NMR (75 MHz, $CDCl_3$) δ (ppm): 16.5 (d, *J* = 5.3 Hz, P(O)OCH_2*C*H_3), 20.1 (d, *J* = 2.3 Hz, P(O)CH_2*C*H_2), 23.5 (d, $^1J_{PC}$ = 140 Hz, P(O)*C*$H_2$$CH_2$), 28.2, 28.3 ($(CH_3)_3C$), 31.4, 32.6 (ArC$H_2CH_2$CH), 49.8 (NC$H_2$$CH_2$), 52.5, 52.5, 52.7, 56.2 (CH_2 ring), 61.3, 61.4 (CH_2COO*t*Bu, OC$H_2$$CH_3$), 64.1 (*C*HCOO*t*Bu), 80.7, 81.0 ($(CH_3)_3C$), 123.6, 129.3, 146.3, 150.2 (Ar*C*), 170.8, 172.3 (*C*(O)). ^{31}P{^{1}H} NMR (122 MHz, D_2O) δ (ppm): 32.8 (s). ESI-HRMS for $C_{41}H_{72}N_5O_{11}P$ $[M + H]^+$, *m*/*z* calcd 842.5038, found 842.5038.

Compound 12. A mixture of **11** (0.45 mg, 0.53 mmol) and 10% Pd–C (90 mg, 20% w/w) in absolute ethanol (20 mL) was shaken under a hydrogen atmosphere (35 psi) in a Parr hydrogenator. After completion of the reaction, the catalyst was removed by filtration through celite and the solvent was removed under reduced pressure. The residue was purified through alumina column chromatography (3% methanol/dichloromethane) to obtain a pure light yellow oil of **12** (0.37 g, 78%).

^{1}H NMR (300 MHz, $CDCl_3$) δ (ppm): 1.29 (t, *J* = 7.5 Hz, 6H, P(O)OCH_2CH_3), 1.35–1.47 (br, 27H, $(CH_3)_3C$), 1.60–1.87 (br, 6H, ArCH_2CH_2CHBr, P(O)CH_2CH_2CH_2), 2.36–2.95 (br, 20H, CH_2 ring), 3.10–3.33 (m, 5H, C*H*COO*t*Bu, CH_2COO*t*Bu) 3.55 (br s, 2H, ArNH_2), 3.93–4.16 (m, 4H, OC$H_2$$CH_3$), 6.60 (d, *J* = 7.5 Hz, 2H, Ar*H*), 6.97 (d, *J* = 7.5, 2H, Ar*H*). ^{13}C{1H} NMR (75 MHz, $CDCl_3$) δ (ppm): 16.4 (d, *J* = 6 Hz, –P(O)–OCH_2*C*H_3), 20.0 (d, *J* = 4.5 Hz, P(O)CH_2*C*H_2CH_2), 23.4 (d, $^1J_{PC}$ = 140 Hz, P(O)*C*H_2*C*H_2CH_2), 28.1, 28.3 ($(CH_3)_3C$), 29.6 (P(O)CH_2*C*H_2CH_2), 31.8 (ArCH_2*C*H_2), 32.3 (Ar*C*$H_2$$CH_2$), 49.7 (N*C*$H_2$$CH_2$), 52.2, 52.3, 52.8, 53.3, 55.6, 55.9 (*C*H_2 ring), 56.13 (*C*H_2COO*t*Bu), 61.3 (d, *J* = 3 Hz, P(O)O*C*$H_2$$CH_3$), 61.3, 64.5 (*C*HCOO*t*Bu), 80.5, 80.5 ($(CH_3)_3C$), 115.1, 129.1, 132.0, 144.2 (Ar*C*), 171.0, 172.8 (*C*(O)). ^{31}P{^{1}H} NMR (122 MHz, $CDCl_3$) δ (ppm): 32.9 (s), 31.0 (s). ESI-HRMS for $C_{41}H_{74}N_5O_9P$ $[M + H]^+$, *m*/*z* calcd 812.5296, found 812.5296.

Ligand L[2]. Bromotrimethylsilane (0.57 mL, 4.31 mmol) was added to a solution of **12** (0.35 g, 0.431 mmol) in anhydrous dichloromethane (15 mL) cooled at 0 °C. The reaction mixture was allowed to warm up to room temperature and was stirred for 16 h. The reaction mixture was concentrated under reduced pressure to remove the excess reagent and solvent. The residue was suspended in anhydrous dichloromethane (15 mL), trifluoroacetic acid (10 mL) was added at 0 °C and the solution was stirred at room temperature for 16 h. The reaction mixture was concentrated under reduced pressure, the residue was dissolved in methanol and added to diethyl ether under vigorous stirring. After filtration and drying, **L[2]** was obtained as an off-white solid (0.21 g, 84%).

^{1}H NMR (300 MHz, D_2O) δ (ppm): 1.53–2.50 (br, 8H, ArCH_2CH_2, P(O)CH_2CH_2CH_2), 2.50–4.0 (br, 23H, CH_2 ring, CH_2COOH and C*H*COOH, NC$H_2$$CH_2$$CH_2$P(O)), 7.34 (d, *J* = 7.5 Hz, 2H, Ar*H*), 7.42 (d, *J* = 7.5 Hz, 2H, Ar*H*). ^{13}C{1H} NMR

(75 MHz, D_2O) δ (ppm): 17.4, 23.9 (d, $^1J_{PC}$ = 135 Hz), 26.4, 31.7, 47.0, 47.3, 47.4, 48.1, 49.4, 49.6, 49.8, 50.2, 53.6, 54.2, 54.5, 61.3, 123.4, 128.3, 130.6, 141.3 (Ar*C*), 171.3, 173.3, 174.5 (*C*=O). $^{31}P\{^1H\}$ NMR (122 MHz, D_2O) δ (ppm): 26.6 (s). ESI-HRMS for $C_{25}H_{42}N_5O_9P$: $[M - H]^-$, *m*/*z* calcd 586.2647, found 586.2643.

Compound 13. 1-Ethyl-3-(3-dimethylaminopropyl) carbodiimide (58 mg, 0.301 mmol) was added to a suspension of biotin (88 mg, 0.36 mmol) and 4-dimethylamino pyridine (76 mg, 0.60 mmol) in anhydrous dimethylformamide (8 mL) at room temperature. The solution of amine **9** (0.23 g, 0.30 mmol) in anhydrous dimethylformamide (6 mL) was added slowly after 10 minutes, and the mixture was stirred for another 16 h. The reaction mixture was concentrated under reduced pressure and the resulting residue was dissolved in dichloromethane (100 mL) and water (100 mL). The organic layer was separated and the aqueous layer was extracted with dichloromethane (2 × 75 mL). The combined organic layers were washed with brine, dried over Na_2SO_4 and concentrated under reduced pressure. The residue was purified by silica gel column chromatography (10% methanol/dichloromethane) to yield product **13** as an off-white solid (0.16 g, 54%).

^1H NMR (300 MHz, $CDCl_3$) δ (ppm): 1.20 (t, *J* = 6 Hz, 6H, (P(O)OCH$_2$C*H*$_3$), 1.26–1.44 (br, 33H), 1.44–1.84 (br, 12H), 1.87–2.60 (br, 13H), 2.61–3.40 (br, 16H,), 3.81–4.06 (m, 4H, OC*H*$_2$CH$_3$), 4.24 (m, 1H, C*H*), 4.39 (m, 1H, C*H*), 5.91 (br s, 1H, N*H*), 6.33 (br s, 1H, N*H*), 8.48 (br s, 1H, N*H*). $^{13}C\{1H\}$ NMR (75 MHz, $CDCl_3$) δ (ppm): 16.2 (d, *J* = 5.3 Hz, P(O)OCH$_2$*C*H$_3$), 18.9, 22.5, 24.4, 25.6, 26.2, 27.6, 27.6, 27.8, 29.0, 35.44, 4.34, 40.4, 44.5, 47.0, 48.1, 49.0, 50.6, 52.3, 53.2, 54.6, 54.8, 55.3, 55.8, 57.0, 59.9, 61.2, 61.3, 61.5, 82.2, 82.2, 83.0, 172.80, 173.6, 173.8, 174.9. ^{31}P NMR (75 MHz, $CDCl_3$) δ (ppm): 26. 6 (s). ESI-HRMS for $C_{47}H_{89}N_7O_{11}PS$: $[M - H]^-$, *m*/*z* calcd 990.6072, found 990.6080.

Compound 14. Following the same procedure as described for compound **13**, compound **14** was isolated as a light yellow solid (98 mg, 56%).

^1H NMR (300 MHz, $CDCl_3$) δ (ppm): 1.28 (t, *J* = 6 Hz, 6H, OCH$_2$C*H*$_3$), 1.40–1.53 (br, 27H, (C*H*$_3$)$_3$C), 1.54–3.73 (br, 39H), 3.91–4.18 (br, 5 H, C*H*COO*t*Bu, OC*H*$_2$CH$_3$), 4.30 (s, 1H, NHC*H*(CH)CH$_2$), 4.48 (s, 1H, NHC*H*(CH)CH$_2$), 5.42–5.88(m, 2H, SC*H*$_2$CH), 7.01 (d, *J* = 6 Hz, 2H, Ar*H*), 7.53 9d, *J* = 6 Hz, 2H, Ar*H*), 8.34 (br, 1H, N*H*). $^{13}C\{1H\}$ NMR (75 MHz, $CDCl_3$) δ (ppm): 14.1, 16.3 (d, *J* = 6 Hz, P(O)OCH$_2$*C*H$_3$), 18.9, 23.4 (d, $^1J_{PC}$ = 135 Hz, P(O)*C*H$_2$*C*H$_2$CH$_2$), 25.5, 27.7, 27.8, 28.0 ((*C*H$_3$)$_3$C), 29.6, 33.4, 36.6, 40.2, 43.9, 47.0, 47.8, 48.5, 50.7, 52.5, 54.6, 54.9, 55.4, 55.9, 56.5, 58.9, 60.4, 61.47, 61.5, 61.9, 82.2, 82.5, 82.9 ((CH$_3$)$_3$*C*), 120.3, 129.0, 135.9, 137.0 (Ar*C*), 164.5, 172.5, 173.0, 174.3, 175.0 (*C*(O)). $^{31}P\{^1H\}$ NMR (122 MHz, $CDCl_3$) δ (ppm): 31.1 (s). ESI-HRMS for $C_{51}H_{89}N_7O_{11}PS$: $[M - H]^-$, *m*/*z* calcd 1038.6072, found 1038.6073.

Ligand L^3. The compound **L^3** was synthesized from **13** following the same procedure as described for **L^2**. The purification was accomplished by RP-HPLC, following the method as described in the Experimental section (0.16 g, 49%).

^1H NMR (300 MHz, D_2O) δ (ppm): 1.01–2.43(br, 18H), 2.49–4.06 (br, 28H), 4.35 (s, 1H), 4.53 (s, 1H). $^{13}C\{1H\}$ NMR (75 MHz, D_2O) δ (ppm): 17.4, 24.1, 25.0 (d, $^1J_{pc}$ = 134 Hz, P(O)*C*H$_2$CH$_2$), 25.2, 25.4, 27.7, 28.0, 28.3, 35.5, 38.6, 39.8, 47.9, 48.2, 49.5, 52.5, 53.1, 53.8, 54.0, 54.3, 54.5, 55.4, 60.2, 62.1, 64.6, 165.2, 172.0, 173.7, 174.6, 176.5 (*C*(O)). $^{31}P\{^1H\}$ NMR (122 MHz, D_2O) δ (ppm): 23.6 (s), 24.0 (s). ESI-HRMS for $C_{31}H_{56}N_7O_{11}PS$: $[M - H]^-$, *m*/*z* calcd 764.3423, found 764.3422.

Ligand L^4. The compound **L^4** was synthesized from **14** following the same procedure as described for **L^2**. The purification was accomplished by RP-HPLC, following the method as described in the Experimental section (68 mg, 58%).

^1H NMR (300 MHz, D_2O) δ (ppm): 1.00–2.00 (br, 12H), 2.00–3.85 (br, 30H), 4.31 (s, 1H), 4.51 (s, 1H), 7.29 (m, 4H). $^{13}C\{1H\}$ NMR (75 MHz, D_2O) δ (ppm): 16.8, 24.8 (d, *J* = 134 Hz, P(O)*C*H$_2$CH$_2$), 25.1, 27.7, 28.0, 29.1, 31.6, 36.2, 39.7, 46.8, 48.7, 48.9, 49.3, 49.5, 50.3, 53.5, 53.8, 55.3, 56.4, 57.5, 60.2, 62.0, 63.5, 122.2, 129.4, 135.2, 137.6 (Ar*C*), 165.2, 173.1, 175.2, 175.2, 175.4 (*C*(O)). $^{31}P\{^1H\}$ NMR (122 MHz, D_2O) δ (ppm): 23.0 (s), 23.7(s). ESI-HRMS for $C_{35}H_{56}N_7O_{11}PS$: $[M - H]^-$, *m*/*z* calcd 812.3423, found 812.3426.

Preparation of Ln^{3+} complexes. **GdL$^{1-4}$** and **EuL$^{1-2}$** were prepared from the respective solution of the ligand (1.0 equiv.) and the aqueous solution of $GdCl_3{\cdot}6H_2O$ for **L$^{1-4}$** or $EuCl_3{\cdot}6H_2O$ (1.0 equiv.) for **L$^{1-2}$**. For each complex the lanthanide salt solution was added portionwise over 6 h. Once no further ligand could be observed by ESI-MS, the reaction mixture was stirred at 60 °C for an additional 16 h. The pH value of the solution was periodically checked and adjusted to 6.5–7.0 by using an aqueous solution of sodium hydroxide (0.5 M). The solutions were then treated with Chelex® 100 sodium form for 4 h at room temperature to remove any excess lanthanide ion. The absence of free Gd^{3+}/Eu^{3+} was confirmed with the xylenol orange test.[32] The complexes were characterized by ESI-LRMS in negative mode and the appropriate isotope pattern distribution for Gd^{3+} and Eu^{3+} was obtained.

Relaxometric experiments

The relaxivities of the complexes **GdL$^{1-2}$** are an average of three measurements at concentrations ranging from 1–3 mM in H_2O. The pH was adjusted with solid LiOH and *p*-TsOH. For each measurement the exact concentration of the Gd^{3+} complex was determined using the bulk magnetic susceptibility shift.

Luminescence steady-state and time resolved experiments

All experiments were performed with 5 mM **EuL$^{1-2}$** at 25 °C. The steady-state measurements were performed in H_2O with the excitation and emission slits set to 1 nm bandpass. The time resolved measurements were performed in H_2O and D_2O. Excitation and emission slits were set to 15 and 5 nm bandpass respectively. Datasets are recorded with a 100 μs delay and 10 μs resolution, and are an average of 15 scans. Each reported value is the mean of three independent measurements and obtained curves are fitted to a first order exponential decay with $R^2 > 0.99$.

Spectrophotometric assay

Stock solutions of avidin and ANS were prepared at concentrations 4 μM and 40 μM, respectively, in 0.15 M sodium phosphate buffer at pH 7. Buffered solutions of avidin (1 mL, 4 μM) and ANS (1 mL, 40 μM) were mixed 1 : 1 (v/v) and the resulting conjugate was titrated with biotin/**GdL^3**/**GdL^4** (320 μM) in 5 μL aliquots. All measurements were performed at 25 °C with the excitation and emission wavelengths of 328 and 408 nm respectively, and excitation and emission slits of 2 nm bandpass.

MRI phantom experiments

MR imaging of the samples was performed at 3T (123 MHz, 21 °C) on a clinical human MR scanner (MAGNETOM Tim Trio, Siemens Healthcare, Germany). Stock solutions of **GdL$^{3-4}$** (0.25 mM) and avidin (0.225 mM) were prepared in HEPES buffer (25 mM, pH 7.4) and water, respectively. The concentration of **GdL$^{3-4}$** was kept constant (0.125 mM) while the concentration of avidin varied up to a ratio of 0.9 avidin–**GdL$^{3-4}$**. The mixtures were kept for 3 h at 37 °C for incubation, followed by the measurement in a 3T MRI scanner. For the subsequent pH-dependent MRI experiments of **GdL$^{3-4}$** with avidin, following buffers were used to adjust pH:MES buffer for pH 5.5 and 6.3, HEPES buffer for pH 7.0, 7.5 and 8.0, and CHES buffer for pH 8.6 and 9.0. The obtained results are mean ± SEM of five independent experiments.

Longitudinal relaxation times (T_1) were measured using an inversion recovery sequence to obtain images from an axial slice of 1 mm thickness through the samples. The inversion time (T_i) was varied from 23 ms to 3000 ms in 12 steps. Images were read out with a turbo spin echo technique, acquiring 5 echoes per scan. The repetition time (TR) was 10 000 ms to ensure complete relaxation. Six averages per T_i were possible within 18 min. For T_2, a home-written spin-echo sequence was used with echo times varying from 25 ms to 275 ms in 10 steps and a repetition time of 8 s. Diffusion sensitivity was reduced by minimizing the crusher gradients surrounding the refocusing pulse. A matrix of 256 × 256 voxels was used over a field-of-view of 110 × 110 mm^2 resulting in a voxel volume of 0.43 × 0.43 × 1 mm^3.

Data analysis was performed by fitting of relaxation curves with self-written routines under MATLAB 7.1 R14 (The Mathworks Inc., United States). The series of T_1 (with varying t = TI) and T_2 (with varying t = TE) relaxation data were fitted to the eqn (2) and (3).

$$S = S_0\ (1 - \exp\ (-t/T_1)) + S_{(\mathrm{TI}=0)}\ \exp\ (-t/T_1) \quad (2)$$

$$S = S_0\ \exp\ (-t/T_2) \quad (3)$$

Nonlinear least-squares fitting of three parameters S_0, $S_{(\mathrm{TI}=0)}$, and T_1/T_2 was done for manually selected regions of interest with the Trust-Region Reflective Newton algorithm implemented in MATLAB. The quality of the fit was controlled by visual inspection and by calculating the mean errors and residuals. The obtained T_1/T_2 values of the samples were converted to R_1 (= $1/T_1$) and R_2 (= $1/T_2$).

$$r_{1,2} = (R_{1,2\mathrm{obs}} - R_{1,2\mathrm{dia}})/[\mathrm{SCA}] \quad (4)$$

Relaxivities r_1/r_2 were calculated by using eqn (4), where $R_{1,2\mathrm{obs}}$ – observed relaxation rate, $R_{1,2\mathrm{dia}}$ – diamagnetic contribution to the relaxation rate and [SCA] – applied concentration of SCA.

Competitive assay

Stock solutions of avidin and **GdL^3**/**GdL^4** were prepared at 0.225 mM and 0.250 mM respectively in HEPES buffer (25 mM, pH 7). A series of different concentrations of biotin were prepared from 250 mM to 1 mM also in HEPES buffer. Avidin (66.7 μL) was mixed with **GdL^3**/**GdL^4** (200 μL) and samples with 0 to 500 times excess of biotin were obtained by adding different volumes of biotin stock solutions 10 min after the preparation of the avidin–**GdL^3**/**GdL^4** mixture. The volume was adjusted to 400 μL by adding HEPES buffer. Mixtures were incubated at 37 °C for 5 h. Longitudinal and transverse relaxation times were recorded on the 3T MRI scanner.

Acknowledgements

The authors thank Dr Sven Gottschalk for help in performing the MRI experiments. We also thank Dr Matteo Placidi, Dr Ilgar Mamedov and Dr Pascal Kadjane for the helpful discussions. The financial support of the Max-Planck Society, German Research Foundation (DFG, grant AN 716/2-1) and German Ministry for Education and Research (BMBF, FKZ: 01EZ0813) is gratefully acknowledged.

Notes and references

1 R. B. Lauffer, *Chem. Rev.*, 1987, **87**, 901–927.
2 J. S. Ananta, B. Godin, R. Sethi, L. Moriggi, X. Liu, R. E. Serda, R. Krishnamurthy, R. Muthupillai, R. D. Bolskar, L. Helm, M. Ferrari, L. J. Wilson and P. Decuzzi, *Nat. Nanotechnol.*, 2010, **5**, 815–821.
3 A. E. Merbach and E. Toth, *The Chemistry of Contrast Agents in Medical Magnetic Resonance Imaging*, Wiley, Chichester, 2001.
4 J. L. Major and T. J. Meade, *Acc. Chem. Res.*, 2009, **42**, 893–903.
5 B. Yoo and M. D. Pagel, *Front. Biosci.*, 2008, **13**, 1733–1752.
6 G. Angelovski and I. Mamedov, *Curr. Inorg. Chem.*, 2011, **1**, 76–90.
7 N. Raghunand, C. Howison, A. D. Sherry, S. R. Zhang and R. J. Gillies, *Magn. Reson. Med.*, 2003, **49**, 249–257.
8 L. M. De Leon-Rodriguez, A. J. M. Lubag, C. R. Malloy, G. V. Martinez, R. J. Gillies and A. D. Sherry, *Acc. Chem. Res.*, 2009, **42**, 948–957.
9 S. R. Zhang, K. C. Wu and A. D. Sherry, *Angew. Chem., Int. Ed.*, 1999, **38**, 3192–3194.

10 M. P. Lowe, D. Parker, O. Reany, S. Aime, M. Botta, G. Castellano, E. Gianolio and R. Pagliarin, *J. Am. Chem. Soc.*, 2001, **123**, 7601–7609.
11 P. Caravan, *Chem. Soc. Rev.*, 2006, **35**, 512–523.
12 S. Aime and P. Caravan, *J. Magn. Reson. Imaging*, 2009, **30**, 1259–1267.
13 M. M. Ali, M. Woods, P. Caravan, A. C. L. Opina, M. Spiller, J. C. Fettinger and A. D. Sherry, *Chem.–Eur. J.*, 2008, **14**, 7250–7258.
14 L. Frullano, C. Catana, T. Benner, A. D. Sherry and P. Caravan, *Angew. Chem., Int. Ed.*, 2010, **49**, 2382–2384.
15 E. Gianolio, R. Napolitano, F. Fedeli, F. Arena and S. Aime, *Chem. Commun.*, 2009, 6044–6046.
16 I. Mamedov, A. Mishra, G. Angelovski, H. A. Mayer, L. O. Palsson, D. Parker and N. K. Logothetis, *Dalton Trans.*, 2007, 5260–5267.
17 N. M. Green, *Methods Enzymol.*, 1990, **184**, 51–67.
18 K. P. Eisenwiener, P. Powell and H. R. Macke, *Bioorg. Med. Chem. Lett.*, 2000, **10**, 2133–2135.
19 Z. Kovacs and A. D. Sherry, *Synthesis*, 1997, 759–763.
20 M. Giardiello, M. P. Lowe and M. Botta, *Chem. Commun.*, 2007, 4044–4046.
21 N. J. Wardle, A. H. Herlihy, P.-W. So, J. D. Bell and S. W. A. Bligh, *Bioorg. Med. Chem.*, 2007, **15**, 4714–4721.
22 D. M. Corsi, C. Platas-Iglesias, H. van Bekkum and J. A. Peters, *Magn. Reson. Chem.*, 2001, **39**, 723–726.
23 A. Beeby, I. M. Clarkson, R. S. Dickins, S. Faulkner, D. Parker, L. Royle, A. S. de Sousa, J. A. G. Williams and M. Woods, *J. Chem. Soc., Perkin Trans. 2*, 1999, 493–503.
24 W. D. Horrocks, J. P. Bolender, W. D. Smith and R. M. Supkowski, *J. Am. Chem. Soc.*, 1997, **119**, 5972–5973.
25 M. Wilchek and E. A. Bayer, *Methods Enzymol.*, 1990, **184**, 5–13.
26 P. Lehtolainen, T. Wirth, A. K. Taskinen, P. Lehenkari, O. Leppanen, M. Lappalainen, K. Pulkkanen, A. Marttila, V. Marjomaki, K. J. Airenne, M. Horton, M. S. Kulomaa and S. Yla-Herttuala, *Gene Ther.*, 2003, **10**, 2090–2097.
27 P. L. Weiden, H. B. Breitz, O. Press, J. W. Appelbaum, J. K. Bryan, S. Gaffigan, D. Stone, D. Axworthy, D. Fisher and J. Reno, *Cancer Biother. Radiopharm.*, 2000, **15**, 15–29.
28 J. Su, F. Chen, V. L. Cryns and P. B. Messersmith, *J. Am. Chem. Soc.*, 2011, **133**, 11850–11853.
29 D. M. Mock, G. Langford, D. Dubois, N. Criscimagna and P. Horowitz, *Anal. Biochem.*, 1985, **151**, 178–181.
30 R. A. Dwek, *Nuclear Magnetic Resonance (N.M.R.) in Biochemistry: Applications to Enzyme Systems*, Clarendon Press, Oxford, 1973.
31 J. B. Livramento, C. Weidensteiner, M. I. M. Prata, P. R. Allegrini, C. Geraldes, L. Helm, R. Kneuer, A. E. Merbach, A. C. Santos, P. Schmidt and E. Toth, *Contrast Media Mol. Imaging*, 2006, **1**, 30–39.
32 B. Paull and P. R. Haddad, *TrAC, Trends Anal. Chem.*, 1999, **18**, 107–114.